Toxicology in Vitro 62 (2020) 104713

Contents lists available at ScienceDirect

Toxicology in Vitro

journal homepage: www.elsevier.com/locate/toxinvit

Interaction of organotin compounds with three major glutathione S-transferases in zebrafish

Ivan Mihaljević[a], Branka Bašica[b], Nikola Maraković[c], Radmila Kovačević[b], Tvrtko Smital[a,*]

[a] Laboratory for Molecular Ecotoxicology, Division for Marine and Environmental Research, Ruđer Bošković Institute, Bijenička 54, 10000 Zagreb, Croatia
[b] University of Novi Sad, Faculty of Sciences, Department of Biology and Ecology, Trg Dositeja Obradovića 2, 21000 Novi Sad, Serbia
[c] Institute for Medical Research and Occupational Health, Ksaverska cesta 2, 10000 Zagreb, Croatia

ARTICLE INFO

Keywords:
Glutathione S-transferases
Zebrafish
Organotin compounds
Type of interaction
Homology modeling
Molecular docking

ABSTRACT

Glutathione S-transferases (GSTs) play an important role in cellular detoxification as enzymatic mediators of glutathione (GSH) conjugation with a wide range of deleterious compounds, enabling their easier extrusion out of the organism. GSTs are shown to interact with organotin compounds (OTCs), known environmental pollutants, either as substrates, serving as electrophilic targets to the nucleophilic attack of GSH, or as noncompetitive inhibitors by binding to GST active sites and disrupting their enzymatic functions. There is a wide range of deleterious biological effects caused by OTCs in low concentration range. Their environmental concentrations, further potentiated by bioaccumulation in aquatic organisms, correspond with inhibitory constants reported for Gsts in zebrafish, which implies their environmental significance. Therefore, our main goal in this study was to analyze interactions of three major zebrafish Gsts – Gstp1, Gstr1, and Gstt1a – with a series of ten environmentally relevant organotin compounds. Using previously developed Gst inhibition assay with recombinant Gst proteins and fluorescent monochlorobimane as a model substrate, we determined Gst inhibitory constants for all tested OCTs. Furthermore, in order to elucidate nature of Gst interactions with OTCs, we determined type of interactions between tested Gsts and the strongest OTC inhibitors. Our results showed that OTCs can interact with zebrafish Gsts as competitive, noncompetitive, or mixed-type inhibitors. Determined types of interactions were additionally confirmed *in silico* by molecular docking studies of tested OTCs with newly developed Gst models. *In silico* models were further used to reveal structures of tested Gsts in more detail and identify crucial amino acid residues which interact with OTCs within Gst active sites. Our results revealed more extensive involvement of Gstr1 and Gstp1 in detoxification of numerous tested OTCs, with low inhibitory constants in nanomolar to low micromolar range and different types of inhibition, whereas Gstt1a noncompetitively interacted with only two tested OTCs with significantly higher inhibitory constants.

1. Introduction

Organotin compounds (OTCs) are organometallic tin-based compounds covalently bound to up to four organic functional groups. Wider commercial use of OTCs as stabilizing agents in polyvinyl chloride (PVC) production started in the 1940s. Later, organotin compounds found more frequent industrial use due to their biocidal properties which made them ideal pesticides and anti-fouling agents (Hoch, 2001). OTCs were used as key components in paints for marine vessels, especially tributyltin (TBT) and triphenyltin (TPhT), which resulted in their higher concentration in aquatic environments. As OTCs are highly toxic compounds with a wide range of deleterious effects on marine life reported at low ng L^{-1} levels (Fent, 1996), more frequent use of highly toxic OTCs was recognized by the World Health Organization and the ban for use of OTCs in anti-fouling paints was declared. However, many countries did not acknowledge the ban and OTC-based paints are still in use in those countries, presenting a significant risk to aquatic environments as well as to human health through diet exposure by eating contaminated marine animals (Fang et al., 2017). Furthermore, even though OTCs are readily degraded in the environment, they have been reported as contaminants in multiple trophic levels (Fent, 1996). In the aquatic environments, the presence of TBT is frequently determined together with its dealkylation products dibutyltin (DBT) and monobutyltin (MBT) (Magi and Di Carro, 2016).

Based on their biological effects, OTCs are classified as endocrine-disrupting chemicals (EDCs). They cause numerous abnormalities in exposed organisms, including morphological and functional changes of reproductive organs. Changes are reported for both genders and range

* Corresponding author.
E-mail address: smital@irb.hr (T. Smital).

https://doi.org/10.1016/j.tiv.2019.104713
Received 20 August 2019; Received in revised form 29 October 2019; Accepted 30 October 2019
Available online 06 November 2019

from lowering of testis and epididymis weights and spermatid count to alteration and damage of the ovaries and uteri. Likewise, OTC exposure and accumulation cause numerous hormonal disturbances in the hypothalamic–pituitary–gonadal axis (de Araújo et al., 2018).

More specifically, toxicity of TBT and its degradation products to fish and other animals has been reported in numerous cases over the last decades. Some examples of TBT damaging effects are brain damage, and notochord and craniofacial deformations in rockfish (*Sebastiscus marmoratus*) (Zhang et al., 2008; 2013), imposex changes in mollusks (Matthiessen and Gibbs, 1998), swimming behavior changes in rainbow trout (*Oncorhynchus mykiss*) (Triebskorn et al., 1994), and activation of phase I detoxication enzymes, *e.g.*, induction of ethoxyresorufin O-deethylase activity in rat hepatoma cells (Kannan et al., 1998). The central nervous system has also been reported as one of TBT targets, where TBT exposure causes a reduction in brain weight and decrease in synaptogenesis, resulting with abnormal behavior in rats (Ema et al., 1991a, 1991b; O'Callaghan and Miller, 1988; Yamada et al., 2010). In addition, oxidative stress was revealed as one of the first events of neuronal cell death caused by TBT exposure in rats (Nakatsu et al., 2006). Reactive oxygen species (ROS) overproduction causes cellular oxidative injury such as lipid peroxidation, protein oxidation, and DNA damage, resulting with cell death, and intracellular signal transduction leading to apoptosis (Droge, 2002). In 2012, Ishihara and colleagues revealed the mechanism by which OTCs cause oxidative stress, showing that TBT treatment of rat hippocampal slices results in inhibition of glutathione S-transferases which in turn causes overproduction of ROS and oxidative injury.

Glutathione S-Transferases (GSTs) are the family of multifunctional enzymes which play an important role in phase II of biotransformation processes (Hayes and Pulford, 1995). Upon entering the cell, deleterious compounds can undergo GST(s)-mediated conjugation with glutathione (GSH) in order to become more polar and more susceptible to extrusion out of the cell or to further biotransformation, thereby averting potential interactions with essential proteins or nucleic acids (Hayes et al., 2005). GSTs are crucial elements in the maintenance of oxido-reductive homeostasis, and as such, they are the key members of secondary defense against oxidative stress. Other known functions of GSTs are steroid isomerization and peroxidation, while some GSTs catalyze biosynthetic reactions of leukotrienes and prostaglandins (Di Giulio and Hinton, 2008).

In detoxification processes, GSTs catalyze nucleophilic attack of an activated thiol group within GSH on electrophilic carbon, nitrogen or sulfur of a xenobiotic substrate (Eaton and Bammler, 1999). GSTs are polyspecific proteins, which interact with numerous types of xenobiotic and endobiotic compounds. Their polyspecificity is achieved due to a flexible structure of the active region with two distinct sites: a hydrophilic, GSH binding site (the G-site), and a hydrophobic, substrate binding site (the H-site). Furthermore, GSTs are catalytically active as homo- and heterodimers as well as monomers, which contributes to their substrate promiscuity (Hayes et al., 2005). Some of the xenobiotic compounds which are conjugated by GSTs are pesticides such as atrazine, DDT, alachlor and lindane (Glisic et al., 2016; Shi et al., 2016; Rossini et al., 1996; Pesce et al., 2008). Carcinogens and their metabolites, such as aflatoxin B1 and benzo(a)pyrene, are also reported as GST substrates (Stewart et al., 1999; Fair, 1986). Some xenobiotics interact with GSTs in a different manner, by non-catalytic binding. This type of binding represents “ligandin” function of GSTs, which enables GST-mediated sequestration and transport of xenobiotics and hormones (Habig et al., 1974; Oakley et al., 1999).

GSTs are classified on the basis of their chemical, physical and structural properties (Sheehan et al., 2001; Wilce and Parker, 1994). There are three GST superfamilies: cytosolic, mitochondrial, and membrane-associated (MAPEG). Based on sequence similarity and structural properties, human cytosolic GSTs are divided into seven classes: alpha, zeta, theta, mu, pi, sigma and omega, some of them with multiple members (Oakley, 2011). Sequence similarities within the class range up to 40%, whereas interclass sequence similarities only go up to 25%. However, despite low sequence similarities, all cytosolic GSTs share universal GST fold (Allocati et al., 2018). As we have shown previously, nine Gst classes are reported in zebrafish, with seven classes of cytosolic Gsts, together with mitochondrial and MAPEG class (Glisic et al., 2015). Gsts are expressed throughout all stages of zebrafish embryonic development as well as in adult organs (Tierbach et al., 2018; Glisic et al., 2015). Although Gsts are ubiquitously expressed in adult zebrafish, three Gst classes – pi, rho, and theta – showed higher expression in toxicologically relevant organs and tissues such as liver, kidney and intestine.

In our previous studies on zebrafish Gsts, we utilized purified recombinant Gstp1, Gstr1, and Gstt1a and showed potent enzymatic activities with model substrates (Glisic et al., 2015; Bašica et al., 2019). We have also demonstrated interactions of different physiological and xenobiotic compounds with a teleost-specific zebrafish Gstr1, including potent interaction with TBT that was characterized as a noncompetitive inhibitor of zebrafish Gstr1 (Bašica et al., 2019). In this study, our main goal was to analyze interactions of three major zebrafish Gsts – Gstp1, Gstr1, and Gstt1a – with a series of ten environmentally relevant organotin compounds. Our specific aims were to identify the most potent Gst inhibitors among tested OTCs, to elucidate their type of interaction, and finally to offer the first insights on the potential significance of these interactions in respect to Gsts-mediated defense against OTCs present in aquatic environments. Our interaction studies and biochemical data were further supported by novel structural models of studied Gsts obtained using homology modeling and *in silico* molecular docking studies.

2. Materials and methods

2.1. Chemicals

All tested OTCs, tributyltin chloride (TBT), tripropyltin chloride (TPrT), triphenyltin chloride (TPheT), triethyltin chloride (TET), methyltin chloride (MET), n-butyltin trichloride (nBT), dimethyltin chloride (DMT), diphenyltin chloride (DPheT), trimethyltin chloride (TMT), dibutyltin chloride (DBT) and other used substrates and compounds were purchased from Sigma-Aldrich (Taufkirchen, Germany) or Alfa Aesar (Ward Hill, MA, USA) unless stated otherwise.

2.2. Inhibition assay

Tested Gst proteins were cloned from zebrafish cDNA and purified as recombinant proteins based on the procedure described previously by Glisic et al. (2015). The inhibition assay was based on the fluorometric assay for GST activity using monochlorobimane (MCB) as a model substrate (Glisic et al., 2015; Bašica et al., 2019). In short, the assay was performed in black, flat bottom 96-well microplates with the final reaction volume of 250 µL at 25 °C. The reaction mix contained 100 mM phosphate buffer (pH 6.5), Gst recombinant protein in the final concentration of 1.5 µg per well, inhibitor at the desired final concentration (or dilution series), GSH in the final concentration of 1 mM, and MCB in the final concentration of 100 µM or in the range of 5–600 µM. The resulting fluorescence was finally determined with the microplate reader (Infinite M200, Tecan, Salzburg, Austria) at 355 nm excitation and 460 nmemission wavelengths for 10 min in 15 s intervals. For blank control, the reaction mixture was prepared without Gst recombinant protein with 100 µL of phosphate buffer. Reaction mixture without a tested compound was used as a positive control, with 100 µL of phosphate buffer.

The first step in determination of inhibition of analyzed Gst enzymes was an initial screening step performed by applying only one, high (100 µM) concentration of tested OTCs. Following the initial inhibition screening, compounds which showed Gst inhibition above 50% were selected for a detailed dose-response studies. Inhibitory potency of each

selected OTC was determined based on determined IC_{50} and K_i values. Inhibition assay for determination of K_i values of tested compounds was based on Michaelis-Menten kinetics of MCB, which was determined by applying MCB substrate in the range of 5–600 μM. MCB dose-response was inhibited with three concentrations of inhibitors based on the determined IC_{25}, IC_{50}, and IC_{75} values. The strength of inhibition of the tested compounds was arbitrarily considered to be very strong for $K_i < 1$ μM, strong for K_i 1–20 μM, moderate for K_i 20–40 μM, and weak for $K_i > 40$ μM.

2.3. Molecular modeling

Biovia Discovery Studio Client v17.2 (Accelrys, San Diego, CA, USA) implemented Build Homology Models protocol was used to construct Gstp1 homology model as based on alignment of the model sequence and the template structure - crystal structure of glutathione S-transferase p1–1 (PDB ID: 19GS) (Oakley et al., 1997). Build Homology Models protocol uses MODELER (Sali and Blundell, 1993) automodel to build homology models. To build Gstr1 homology model, the input sequence alignment between the model sequence of Gstr1 monomer and the sequence of chain A glutathione S-transferase p1–1 was obtained using AlignSequenceProfiles (MODELER protocol). Rest of the parameters in the Parameters Explorer of Build Homology Models protocol were set as described previously (Mihaljevic et al., 2017). Ligands to be docked in the homology model of Gstr1 were created with ChemBio3D Ultra 13.0 (PerkinElmer, Inc., Waltham, MA, USA) and minimized using the MMFF94 force field implemented in ChemBio3D Ultra 13.0. Biovia Discovery Studio Client v17.2 implemented FlexibleDocking protocol (Koska et al., 2008) was used for the docking study which docks ligands into a receptor with flexible amino acid side-chains while the following steps are performed: receptor conformations calculation using ChiFlex, creation of ligand conformations, docking of the ligand into each active protein conformation site using LibDock, clustering of the poses to remove similar ligand poses, rebuilding of the protein conformations by refining selected protein side-chains in the presence of the rigid ligand using ChiRotor, and a final ligand refinement using CDOCKER. The homology model with the highest overlay similarity was used as the rigid receptor, while the binding site within the homology models was defined by a sphere ($r = 14.5$ Å) surrounding the amino acids that have been located within the identified G- and H-site. For more details about parameters in FlexibleDocking protocol, the reader is referred to Supplementary Material. The binding affinities of docked ligands in the poses generated by FlexibleDocking protocol were estimated using the scoring functions as implemented in the Biovia Discovery Studio Client v17.2 ScoreLigandPoses protocol followed with ConsensusScore protocol, as described previously (Bašica et al., 2019). The representative poses of docked ligands with the highest consensus score were minimized using Biovia Discovery Studio Client v17.2 Minimization protocol, as described elsewhere (Marakovic et al., 2016).

2.4. Data analysis

All assays were performed in three independent experiments run in triplicates. Data shown on related figures represent mean ± standard errors of mean (SEM). All calculations were performed using GraphPad Prism 6.00 for Windows (GraphPad Software, San Diego, CA, USA) as described below. The kinetic parameters, K_m and V_{max} values were calculated using the Michaelis-Menten Eq (1):

$$V = \frac{Vmax \times [S]}{[S] + Km} \quad (1)$$

where V is velocity (fluorescence units per milligram of protein per minute), V_{max} is maximal velocity, [S] is substrate concentration and K_m is Michaelis–Menten constant.

For the purpose of K_i determination, the obtained data were analyzed by nonlinear regression, mixed-model enzyme inhibition. The used GraphPad model provided the alpha value (α) which is an indication of the type of interaction of the tested compounds with selected zebrafish recombinant proteins. The alpha value determines the level to which the inhibitor changes the affinity of the enzyme for the model substrate. In the case of alpha equals 1, the inhibitor does not affect the binding of substrate to the enzyme which results in non-competitive inhibition. When alpha equals much higher number than 1, binding of the inhibitor blocks binding of the substrate resulting in competitive inhibition (Copeland, 2005). Furthermore, when alpha value is slightly higher than 1 in a range up to 30, together with recorded changes in increase of K_m and decrease of V_{max}, it suggests more complex interaction between an enzyme and interactor, which can be defined as mixed type of inhibition.

3. Results

The initial step in characterizing the interaction between zebrafish recombinant proteins, Gstr1, Gstp1, and Gstt1a, and organotin compounds performed with only one concentration of tested OTCs (set at 100 μM) revealed potent interactions of Gstr1 with TBT, TPrT, triphenyltin chloride (TPheT), triethyltin chloride (TET), diphenyltin chloride (DPheT), and DBT, all resulting in at least 90% of inhibition of the enzyme activity (Fig. 1). The similar inhibitory pattern was revealed for inhibition of Gstp1, with the difference in DBT inhibition, which showed inhibition of Gstp1 activity of only 26%. Gst1a exhibited different inhibition pattern, with only two OTCs causing inhibition above 50%: methyltin chloride (MET) with 77% and DPheT with 64%, respectively (Fig. 1).

In order to quantify the potency of determined Gst inhibition in more detail, we proceeded with the determination of IC_{50} values for each compound that showed inhibition above 50% in the initial screening. DPheT exhibited the most potent inhibition of Gstr1, with IC_{50} value 0.08 μM, followed by DBT, TBT, TPrT and TPheT which showed inhibition in a similar range (Table 1, Supplementary Fig. S1). With IC_{50} value of 2.65 μM, TET showed the lowest inhibitory potential towards zebrafish Gstr1. Inhibition of Gstp1 was highest with TPrT, with IC_{50} of 0.18 μM, followed by TPheT, TET, and TBT, with IC_{50} values in similar range (Table 1, Supplementary Fig. S2). DPheT showed the lowest inhibitory potential for Gstp1, with IC_{50} of 24.96 μM. Only two tested organotin compounds, MET and DPheT, inhibited Gstt1a, which resulted with IC_{50} values of 28.4 μM and 68.1 μM, respectively (Table 1, Fig. S3).

Determination of the type of interaction was based on the determination of K_i and alpha (α) values, together with the observation of Michaelis-Menten kinetics of K_m and V_{max} values. Determined K_i values

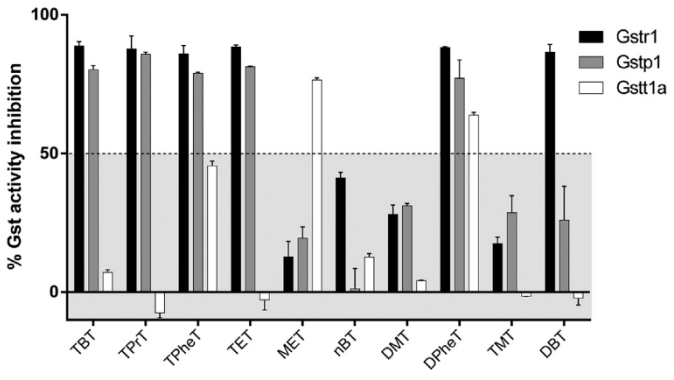

Fig. 1. Interaction of zebrafish Gstr1, Gstp1, or Gstt1a with organotin compounds. Data are expressed as percentage (%) of the inhibition of respective Gst activity towards model fluorescence substrate monochlorobimane (MCB; 100 μM) in presence of each modulator (100 μM) and co-substrate glutathione (GSH; 1 mM) relative to activity in absence of a modulator. Data represent mean ± SEM of triplicates from three independent experiments.

Table 1
IC_{50} values with 95% confidence intervals determined for tested OTCs which showed inhibition above 50% with zebrafish Gstr1, Gstp1, and Gstt1a.

Enzyme	Compound	IC_{50} (μM)	c.i. (95%)
Gstr1	DPheT	0.08	0.07 to 0.09
	TBT	0.09	0.08 to 0.10
	DBT	0.09	0.08 to 0.11
	TPrT	0.1	0.08 to 0.12
	TPheT	0.18	0.13 to 0.24
	TET	2.65	1.69 to 4.14
Gstp1	TPrT	0.18	0.13 to 0.26
	TPheT	1.48	0.89 to 2.48
	TET	3.54	1.32 to 9.48
	TBT	3.67	2.18 to 6.19
	DPheT	24.96	22.76 to 27.38
Gstt1a	MET	28.44	24.26 to 33.34
	DPheT	68.09	51.97 to 89.22

revealed most of tested OTCs as very strong inhibitors of Gstr1, except for TET and TPrT which were determined as strong inhibitors (Table 2). TPrT and DPhet showed to be very strong inhibitors of Gstp1, whereas other tested OTCs showed strong inhibition, with slightly higher K_i values (Table 2). Finally, both tested OTCs, Met and DPheT, showed as strong inhibitors of Gstt1a (Table 2). Based on all tests applied, three types of interactions were determined between tested OTCs and zebrafish Gstr1, Gstp1 or Gstt1a: competitive, noncompetitive and mixed-type inhibition. Considering determined α values, clear noncompetitive inhibition of Gstr1 was determined for TBT, TPheT, and DPheT, while other compounds exhibited higher, although not exceptionally high α values, which indicated potential competitive, or a mixed-type of inhibition (Table 2, Fig. 2, Supplementary Fig. S4). The only two examples of noncompetitive inhibition of Gstp1 were determined for TBT and DPheT, and other tested OTCs showed potential competitive or mixed-type inhibition (Table 2, Fig. 2, Supplementary Fig. S4). Finally, both tested inhibitors of Gstt1a, MET and DPheT, were characterized as noncompetitive inhibitors (Table 2, Supplementary Fig. S4).

As the method for determination of the type of interaction based on α values generated some inconclusive results in the form of mixed-type inhibition, we performed additional Michaelis-Menten kinetics analysis. Therefore, based on changes in enzyme kinetics constants K_m and V_{max} we determined the type of interaction between OTCs compounds and tested Gst enzymes. Using data obtained with this approach, we deduced that TET, TPrT and DBT are competitive inhibitors of Gstr1, DPheT is a noncompetitive inhibitor, whereas TPheT showed mixed-type of inhibition due to the change in both constants, *i.e.* raise of K_m and lowering the V_{max} (Table 3). Michaelis-Menten analysis of zebrafish Gstp1 kinetics with tested OTCs revealed TPrT, TBT and TPheT as competitive inhibitors, DPheT as a noncompetitive inhibitor, whereas TET showed mixed-type of inhibition (Table 3, Supplementary Fig. S4). For Gstt1a, both interacting OTCs (MET and DPheT) were confirmed as noncompetitive inhibitors (Table 3).

3.1. Homology modeling of Gstp1

Recently, we have reported results on molecular docking studies obtained using zebrafish Gstr1 three-dimensional (3D) homology model to support experimentally determined results with various endogenous and exogenous compounds (Bašica et al., 2019). In this work, we used the same approach refined with new substrates and 3D homology model of zebrafish Gstr1 (Fig. 3A) and Gstp1 (Fig. 4A). Homology model of Gstp1 was constructed *de novo*, the template structure was chosen based on the highest indexes of sequence identity and sequence similarity, and finally, crystal structure of glutathione S-transferase p1–1 (PDB ID: 19GS) (Oakley et al., 1997) was chosen (sequence identity 59.5% and sequence similarity 81.4%). The binding site of the final dimeric model structure of zebrafish Gstp1 was defined and edited using both the software features that automatically identify cavities within the receptor and knowledge on residues that constitute glutathione-binding site (G-site) and hydrophobic substrate-binding site (H-site), which are largely conserved within the same GST classes. Thus, by sequence alignment of zebrafish pi class Gstp1 and human GSTP1–1, we identified the residues forming the G-site (Tyr8, Phe9, Val11, Gly13, Arg14, Cys15, and Tyr109) and the H-site (Ala10, Phe36, Ile205, Pro201, and Gly204). In addition, homology model of Gstp1 with GSH occupying G-site was obtained after structural alignment between model structure of Gstp1 and crystal structure of the human GSTP1–1 in complex with GSH (PDB ID: 5GSS) (Oakley et al., 1997) followed by hard docking of the GSH to the model structure of Gstp1 (Fig. 4A).

3.2. Molecular docking studies

To support kinetic measurements and elucidate binding modes and types of interaction between tested OTCs and Gstr1 and/or Gstp1, we performed molecular docking studies using above mentioned homology models. For maximum simulation credibility, the FlexibleDocking protocol was used which allows for the simulation of protein flexibility and docking of ligands with an induced fit receptor optimization (Koska et al., 2008). The residues selected for flexible docking, *i.e.* creating protein conformations and side-chain refinement in the presence of ligands, were chosen from within the binding sphere to include residues presumed to interact with studied ligands. Choice of ligands to be docked was made such to cover all types of inhibition as indicated with kinetic studies. In Fig. 3A, a 3D homology model of zebrafish Gstr1 with GSH inside the binding site used as a receptor for flexible docking is

Table 2
Inhibition constants (K_i) determined for tested OTCs towards zebrafish Gstr1, Gstp1, and Gstt1a. Type of interactions, alpha (α) values, 95% confidence intervals and coefficients of determination are shown.

Enzyme	Compound	Inhibition type	α	K_i (μM)	95% c.i.	R^2
Gstr1	TET	Competitive/mixed	23.8 ± 15.2	1.27 ± 0.18	0.9–1.6	0.98
	TPrT	Noncompetitive	5.3 ± 1.6	5.25 ± 0.02	0.1–0.17	0.99
	TBT[a]	Noncompetitive	1.2 ± 0.6	0.26 ± 0.0.2	0.21–0.31	0.93
	TPheT	Noncompetitive	1.7 ± 0.8	0.07 ± 0.02	0.02–0.12	0.99
	DBT	Noncompetitive	4.9 ± 1.6	0.07 ± 0.01	0.05–0.1	0.99
	DPheT	Noncompetitive	1.4 ± 0.7	0.06 ± 0.02	0.02–0.09	0.99
Gstp1	TET	Competitive/mixed	15.0 ± 16.3	1.32 ± 0.21	0.9–1.7	0.99
	TPrT	Competitive/mixed	30.1 ± 79.2	0.9 ± 0.15	0.6–1.2	0.98
	TBT	Noncompetitive	6.8 ± 4.2	1.9 ± 0.3	1.3–2.5	0.99
	TPheT	Competitive/mixed	18.1 ± 82.9	19.6 ± 6.9	5.7–33.5	0.97
	DPheT	Noncompetitive	2.5 ± 2.3	0.7 ± 0.3	0.1–1.3	0.97
Gstt1a	MET	Noncompetitive	0.64 ± 0.3	8.4 ± 2.5	3.5–15.4	0.99
	DPheT	Noncompetitive	1.4 ± 0.7	5.2 ± 1.3	2.5–7.9	0.99

[a] Type of interaction for TBT was determined previously (Bašica et al., 2019)

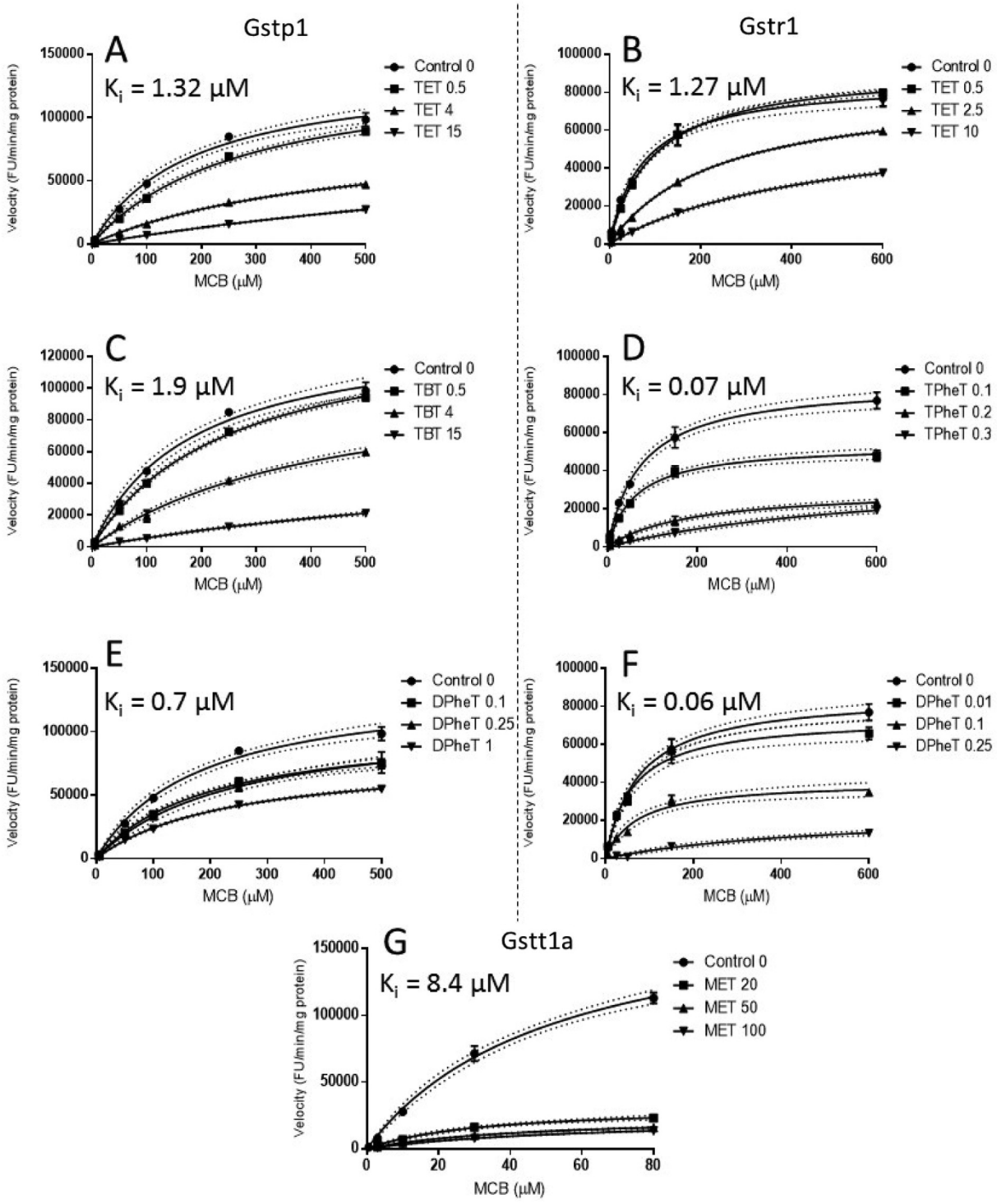

Fig. 2. Example of dose-response curves used to determine the type of interaction based on changes in K_m and V_{max} constants for Gstr1, Gstp1, and Gstt1a. A) TET (0.5, 4 and 15 µM) as a mixed type inhibitor of Gstp1, B) TET (0.5, 2.5 and 10 µM) as a competitive inhibitor of Gstr1, C) TBT (0.5, 4 and 15 µM) as competitive inhibitor of Gstp1, D) TPheT (0.1, 0.2 and 0.3 µM) as mixed type inhibitor of Gstr1, E) DPheT (0.1, 0.25 and 1 µM) a noncompetitive inhibitor of Gstp1, F) DPheT (0.01, 0.1 and 0.25 µM) as a noncompetitive inhibitor of Gstr1, G) MET 20, 50 and 100 (µM) as a noncompetitive inhibitor of Gstt1a. Each data point represents the mean ± SD from a typical experiment out of three independent determinations. Dotted lines represent 95% confidence intervals.

shown, as deduced from the crystal structure. For the representative pose, top-scored pose was chosen as determined using ScoreLigandPose and ConsensusScore protocols designed to estimate binding affinities towards docked ligands, as described previously (Bašica et al., 2019). Model complex obtained with docking of TET into Gstr1-GSH shows that TET is predicted to bind in an orientation that fulfills all pre-requisites for successful in-line nucleophilic attack from thiol group of GSH molecule: Sn atom is open for approach of thiol group; Sn atom is 4.7 Å from thiol group – a distance close enough for reactivating groups in pre-reactionary complex for nucleophilic attack; and finally – Cl atom, that is supposed to be leaving group in the reaction mechanism, lies in line with thiol group and Sn atom. This is in accordance with kinetic results which describe TET as a competitive inhibitor. In addition, TET is stabilized through multiple hydrophobic π-alkyl non-

Table 3
Determination of the type of interaction for tested OTCs (IC_{50} values) with zebrafish Gstr1, Gstp1, and Gstt1a. Kinetic parameters of MCB-GSH conjugation are given as K_m (μM), V_{max} (FU/mg protein/min), and 95% confidence intervals for each.

Enzyme	Compound	Inhibition type	K_m (μM)	95% c.i.	V_{max} (FU/mg protein/min)	95% c.i.
Gstr1	Control	–	74.9 ± 7.4	57.9 to 92.0	86,286 ± 2778	79,879 to 92,693
	TET	Competitive	237.1 ± 6.5	222.0 to 252.2	83,138 ± 971	80,898 to 85,378
	TPrT	Competitive	140.0 ± 10.5	115.8 to 164.1	68,967 ± 1920	64,540 to 73,393
	TPheT	Mixed	183.1 ± 26.3	122.5 to 243.8	30,390 ± 1729	26,404 to 34,376
	DBT	Competitive	124.4 ± 11.7	97.5 to 151.3	69,044 ± 2349	63,626 to 74,461
	DPheT	Noncompetitive	71.6 ± 12.8	42.0 to 101.2	40,475 ± 2341	35,076 to 45,875
Gstp1	Control	–	180.6 ± 22.5	128.8 to 232.4	137,609 ± 7071	121,303 to 153,915
	TET	Mixed	459.6 ± 37.5	373.2 to 546.0	90,635 ± 4237	80,864 to 100,406
	TPrT	Competitive	477.1 ± 30.4	407.0 to 547.2	158,185 ± 5853	144,687 to 171,682
	TBT	Competitive	434.2 ± 58.6	298.3 to 570.1	112,210 ± 8573	92,440 to 131,980
	TPheT	Competitive	325.0 ± 28.1	260.2 to 389.7	189,002 ± 8320	169,816 to 208,188
	DPheT	Noncompetitive	235.2 ± 13.8	203.4 to 266.9	81,012 ± 2152	76,049 to 85,975
Gstt1a	Control	–	51.9 ± 6.4	37.1 to 66.8	187,796 ± 11,591	161,066 to 214,525
	MET	Noncompetitive	44.0 ± 3.9	35.0 to 53.0	24,770 ± 1028	22,398 to 27,141
	DPheT	Noncompetitive	62.2 ± 16.5	24.3 to 100.2	51,454 ± 7229	34,784 to 68,124

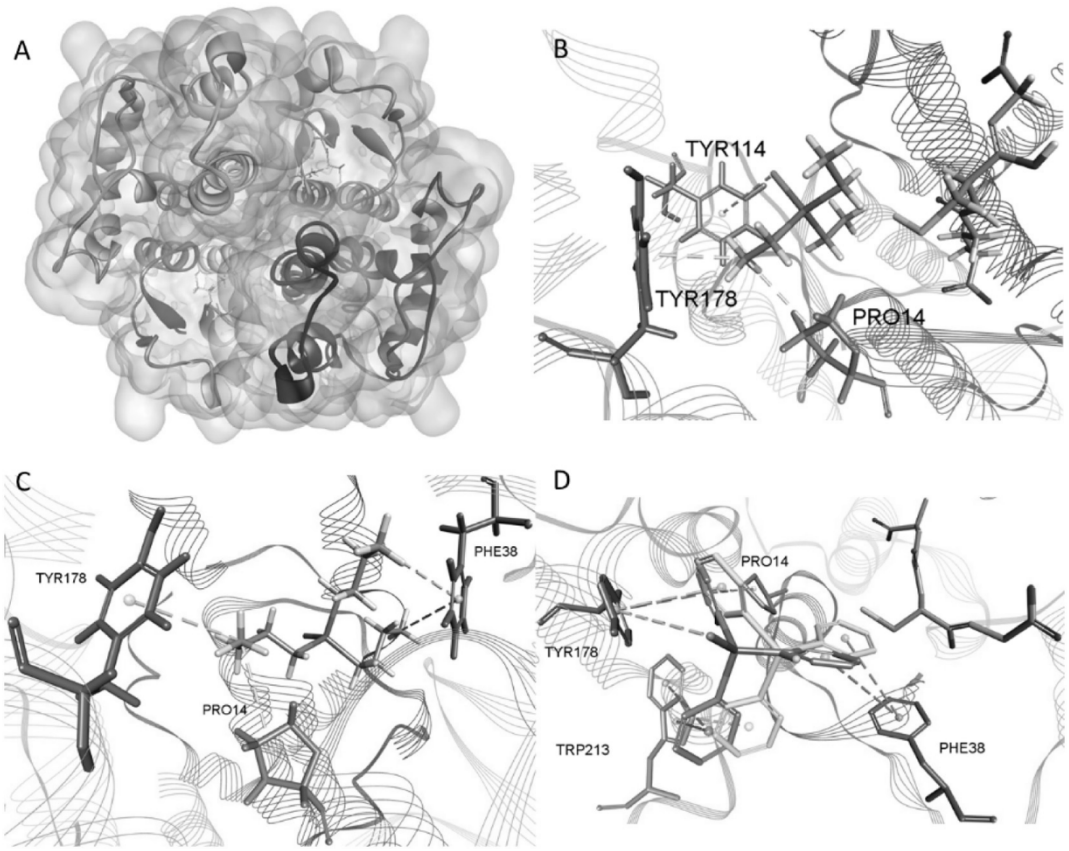

Fig. 3. A) Final 3D structure of zebrafish (*Danio rerio*) rho class Gstr1 with docked GSH in each monomer G-site. B) Final docking pose of the TET-GSH-Gstr1 complex and close-up view of the active site residues. C) Final docking pose of the TPrT-Gstr1 complex and close-up view of the active site residues. D) Final docking pose of the TBT-Gstr1/GSH-Gstr1 complex and close-up view of the active site residues. TBT docked in Gstr1 is shown in yellow. In all figures non-bonding interaction are shown in purple dotted lines. (For interpretation of the references to colour in this figure legend, the reader is referred to the web version of this article.)

bonding interactions with known H-site residue Pro14 together with Tyr114 and Tyr178.

Fig. 3D shows the model complex obtained with the docking of TBT into zebrafish Gstr1. In accordance with kinetic results that suggest that TBT is a noncompetitive inhibitor, TBT is predicted to bind in a position where it significantly affects the binding of GSH molecule by protruding into G-site, thus preventing binding of GSH. In doing so, TBT engages into multiple hydrophobic π-alkyl interactions with G-site residue Pro14, together with Phe38 and Tyr178. Finally, model complexes obtained with docking of TBT into Gstr1-GSH and Gstr1 as shown in Fig. 3D illustrate how mixed-type inhibition could result from two distinctive binding modes predicted for Gstr1-GSH (TBT colored in silver) and Gstr1 (TBT showed in yellow), both with two highest consensus scores among all generated poses in this work. While TBT docked in Gstr1-GSH is positioned so that it can undergo nucleophilic attack from thiol group of GSH with leaving group, *i.e.* Cl atom directed opposite of the thiol group, TBT docked in Gstr1 is slightly shifted towards the G-site, but enough to cause steric clash with bound GSH molecule, thus implying that in this position TBT prevents binding of GSH molecule. To sum up, firstly described docking pose refers to a competitive mode of inhibition of TBT, while the second pose describes a noncompetitive mode of inhibition of TBT. Interestingly, in both

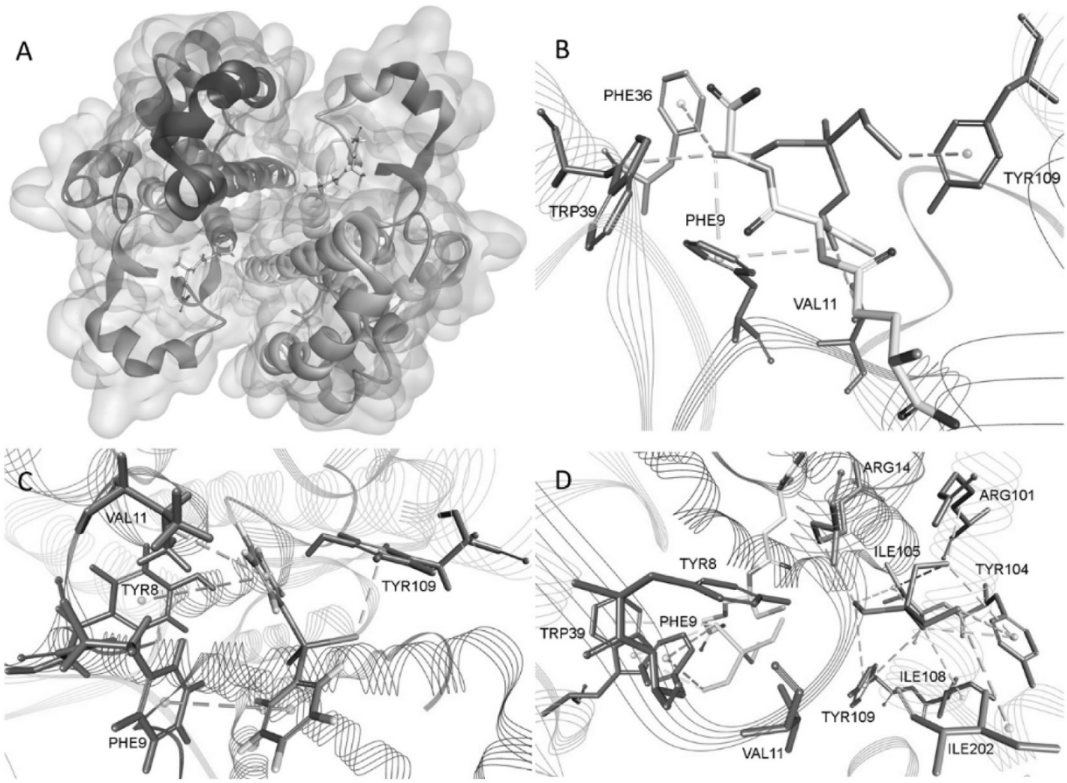

Fig. 4. A) Final 3D structure of zebrafish (*Danio rerio*) pi class Gstp1 with docked GSH in each monomer G-site. B) Final docking pose of the TPrT-GSH-Gstp1 complex and close-up view of the active site residues. C) Final docking pose of the DPheT-Gstp1 complex and close-up view of the active site residues. D) Final docking pose of the TET-Gstp1/GSH-Gstp1 complex and close-up view of the active site residues. TET docked in Gstp1 is shown in yellow. In all figures non-bonding interaction are shown in purple dotted lines. (For interpretation of the references to colour in this figure legend, the reader is referred to the web version of this article.)

cases, TBT is stabilized through multiple hydrophobic π-alkyl interactions with the same residues: Pro14, Phe38, Tyr178, and Trp213.

In analogy with the presentation of docking results with Gstr1 homology model, we present the results of molecular docking studies with a homology model of zebrafish Gstp1 (Fig. 4A), covering all types of inhibition determined with kinetic measurements. Indeed, model complex obtained with docking of TPrT into GSH-Gstp1 shows TPrT in position prior to nucleophilic attack by thiol group of GSH molecule stabilized through multiple hydrophobic π-alkyl interactions with known G-site residues Phe9 and Val11, and H-site residues Phe36, Trp39, and Tyr109 which is known for its multifunctional role in the catalytic mechanism of human GSTP1–1 (Lo et al., 1997)

On the other hand, model complex obtained with the docking of noncompetitive inhibitor DPheT into Gstp1 (Fig. 4C) shows DPheT occupying G-site interacting with surrounding known G-site residues (Tyr8, Phe9, and Val11) and Tyr109, thus blocking binding of GSH molecule. Finally, mixed-type inhibitor TET is predicted to bind both susceptible to nucleophilic attack (competitive mode) and protruding into G-site (noncompetitive mode) as shown in Fig. 4D.

4. Discussion

Glutathione S-transferases are important elements of cellular detoxification system in aquatic organisms. Impairment of their normal function enhances the susceptibility of an organism to numerous toxic pollutants and is consequently linked to deleterious effects such as oxidative stress, carcinogenicity, and acute or chronic toxicity (Sheehan et al., 2001). Therefore, determinations of GST expression and activity has been widely applied and established as environmental biomarker through decades of research (Luk'yanova and Ireikina, 2011). Consequently, it is of great significance to have a detailed insight into identities, expression patterns, substrate specificities, catalytic mechanisms and structural properties of Gsts in zebrafish as a widely used model organism. In recent studies, the presence of different classes of Gsts in zebrafish has been showed, their tissue expression profiles established, and basic enzyme kinetic properties determined (Glisic et al., 2015; Tierbach et al., 2018). Fifteen identified and annotated genes of cytosolic Gsts in zebrafish, distributed in seven classes, showed ubiquitous tissue expression, with high expression of Gst pi, rho and theta class in liver, kidney, and intestine as toxicologically most relevant tissues (Glisic et al., 2015). Purified recombinant zebrafish Gsts showed potent catalytic activities with model substrates, 1-chloro-2,4-dinitro benzene (CDNB), monochlorobimane (MCB), etacrynic acid (ETA), dichloroacetic acid (DCA) and dehydroascorbate (DHA) (Glisic et al., 2015).

Our functional characterization of recombinant zebrafish Gsts served as a basis for the development of screening and interaction assays that were used for further analyses of interactions of Gsts with different environmental pollutants and physiologically relevant compounds. Considering that zebrafish Gstr1 showed potent interactions with several industrial contaminants, and TBT was shown to be a highly potent Gstr1 inhibitor with the K_i value of 0.26 μM (Bašica et al., 2019), in this study we analyzed in more detail members of three major cytosolic Gst classes in zebrafish – Gstr1, Gstp1, and Gstt1a – in respect to their interactions with organotin compounds. Our aim was to deduce the inhibitory potencies of each of ten selected OTC members and determine the types of interactions of OTCs with selected zebrafish Gsts. Finally, interactions observed experimentally for each of the tested OTCs were additionally evaluated using *in silico* analysis based on homology modeling and molecular docking studies.

Gstr1 is the only member of the teleost-specific rho class of cytosolic Gsts in zebrafish (Glisic et al., 2015; Tierbach et al., 2018). It is highly expressed in kidney, brain, liver and intestine, suggesting possible involvement in physiological functions such as steroidogenesis and

metabolism of steroid hormones and bile salts (Glisic et al., 2015; Bašica et al., 2019). Six OTC members – TET, TPrT, TBT, TPheT, DBT and DPheT – are identified in this study as potent Gstr1 inhibitors (Fig. 1), and resulting K_i values ranged from nanomolar to low micromolar concentrations (Table 2). Comparison of Gstr1 inhibitory concentrations obtained in this study with environmental concentrations of some of the tested OTCs, as well as reported tissue accumulation concentrations ranging up to 2.5 μg of Sn per gram of dry weight, emphasizes potential significance of Gstr1 in defense against harmful effects of environmentally available OTCs (Stäb et al., 1996; Antizar-Ladislao, 2008). However, Gstr1 showed different types of interactions with tested OTCs. It reveals complex interactions with these deleterious compounds, which can result not only with nucleophilic attack and GSH conjugation of OTC, but also with non-enzymatic bonding with Gstr1 (Tables 1 and 2). TET and TPrT are shown to be competitive inhibitors of zebrafish Gstr1, implying the involvement of Gstr1 in their conjugation with GSH. Sterically, they can be placed and stabilized within active sites of Gstr1, facilitating in-line nucleophilic attack of GSH (Fig. 3B and C). Other OTCs interacted with Gstr1 by non-competitive and mixed-type inhibition. Their placement within Gstr1 G- and H-active sites, along with disruption of crucial amino acid residues of both sites, results with unfavorable conditions for in-line nucleophilic attack thus blocking the catalytic function of Gstr1. Furthermore, strong inhibitory interactions suggest that low concentrations of environmentally present OTCs may affect the detoxifying function of Gstr1. From a different perspective, Gst interaction with certain compounds can be non-catalytic and it is possible that Gstr1 have a scavenging role, *e.g.*, by showing "ligandin" binding properties with OTCs to prevent their deleterious effects on crucial biological structures such as proteins and nucleic acids (Oakley et al., 1999). Overall, taking into account its high expression in toxicologically relevant tissues, and the type and potency of investigated interactions, zebrafish Gstr1 enzyme can have a significant role in protection against harmful effects of OTCs.

Similarly, Gstp1 showed ubiquitously high expression in zebrafish liver, intestine, and gills, suggesting its toxicological significance (Glisic et al., 2015; Tierbach et al., 2018). Catalytically, Gstp1 showed similar activity towards model substrates as Gstr1 which additionally implied an important role of Gstp1 against deleterious environmental contaminants (Glisic et al., 2015). TPrT showed to be the most potent competitive inhibitor of Gstp1 among tested OTCs, with K_i value of 0.9 μM, whereas the weakest inhibition was obtained with TPheT with K_i value of 19.6 μM (Table 2). Furthermore, in this study we showed, both by biochemical analyses and molecular docking *in silico*, that TPrT, TBT and TPheT are competitive inhibitors of Gstp1 (Fig. 4, Table 3). Molecular docking showed the favorable placement of studied OTCs and interactions with crucial amino acid residues of Gstp1 active sites to achieve in-line nucleophilic attacks of GSH and consequently enable successful detoxification of these compounds. Gstp1 showed mixed-type of inhibition by TET, indicating different catalytic properties than Gstr1 which showed conjugating capabilities with TET acting as a competitive inhibitor (Tables 2 and 3). Molecular docking of TET within active sites of Gstp1 revealed two distinctive modes of interaction, suggesting a more complex interaction that results in changes of both catalytic constants by lowering the affinity of Gstp1 towards TET, and in the same time lowering the Vmax (Table 3, Fig. 4D). Inhibition of Gstp1 by tested OTCs obtained in low micromolar range suggests its importance in detoxifying processes. Moreover, OTCs present in the environment may have a deleterious effect on the proper functioning of Gstp1 towards other xenobiotic or endobiotic substrates. Similarly to reported OTC inhibition, human GSTP1 is inhibited in low micromolar range with organometallic compounds containing ruthenium and osmium (Păunescu et al., 2017). Human GSTP1 is also inhibited by organic methylmercury and selenium in the micromolar range (Goodrich and Basu, 2012). Taking together, our data showing interactions of zebrafish Gstp1 with OTCs, along with reported interactions of human GSTP1 and other non-mammalian Gst members, suggest a conserved defensive role of Gsts against organometallic compounds and heavy metals in the environment.

Gstt1a exhibited highly potent catalytic activity towards model substrates, especially MCB, which was conjugated by this enzyme with high speed and affinity (Glisic et al., 2015). However, in this study Gstt1a showed the weakest interactions with tested OTCs. Initial OTC interaction screening revealed only MET and DPheT as relatively potent Gstt1a inhibitors (Fig. 1). Our further analyses resulted in determined K_i values for MET and DPheT of 8.4 μM and 5.2 μM, respectively, in the range of values determined for OTC inhibitions with other Gsts (Table 2). Furthermore, both investigated OTC Gstt1a interactors showed to be noncompetitive inhibitors, implying that Gstt1a potentially does not have an active role in the conjugation of OTCs and their subsequent excretion. Taking into account moderate expression of Gstt1a in liver and kidney, with exception of high expression in male liver, it can be presumed that Gstt1a potentially plays an important role in steroidogenesis, as it was reported with other GST classes such as human GSTA3–3 (Johansson and Mannervik, 2002). However, it probably has a rather minor role in GSH conjugation-based toxicological defense, although non-catalytic scavenging interactions of deleterious compounds cannot be excluded, as shown with non-competitive inhibition of MET and DPheT.

In conclusion, in this study we showed that environmentally relevant OTCs are potent interactors with zebrafish Gsts, implying the importance of Gst-based defense against OTCs as part of phase II of cellular detoxification. Taking into account the presence of OTCs in aquatic environments, their inhibitory potential towards Gsts has to be considered. Furthermore, novel structural and mechanistic insights on interactions between zebrafish Gsts and OTCs are provided. Molecular docking studies of Gstr1 and Gstp1 confirmed catalytic properties initially determined through biochemical analyses, and revealed in more detail steric and mechanistic interactions of tested OTCs with amino acid residues within G- and H-active sites. Our findings on different types of inhibition suggest that some OTCs are competitive inhibitors (*i.e.* substrates) of zebrafish Gsts which can thus carry out their catalytic role and contribute to further metabolism and extrusion of OTCs out of the organism. On the other hand, OTCs showing a noncompetitive, or a mixed-type of inhibition could be handled by Gsts differently, *e.g.*, by non-catalytic binding, preventing further damage to crucial biological structures. Our results further showed that Gstr1 and Gstp1 have a more complex nature of interaction with OTCs, which can inhibit Gst activities by three different types of inhibition. On the other side, Gstt1a interacted with two tested OTCs only, which inhibited Gstt1a as non-competitive inhibitors, suggesting that Gstt1a can possibly have only "ligandin" functions by binding and sequestering OTCs. Finally, due to the scarcity of studies focused on detailed functional characterizations of non-mammalian Gsts, this study provides a basis for further *in vivo* studies aimed at deciphering defensive and physiological functions of Gsts in zebrafish.

Declaration of Competing Interest

The authors declare that they have no known competing financial interests or personal relationships that could have appeared to influence the work reported in this paper.

Acknowledgements

This research was financed by the SCOPES joint research project supported by Swiss National Science Foundation (SNSF) (Grant No. SCOPES - IZ73ZO_152274/1), and partially supported under the project STIM – REI, Contract Number: KK.01.1.1.01.0003, a project funded by the European Union through the European Regional Development Fund – the Operational Programme Competitiveness and Cohesion 2014-2020 (KK.01.1.1.01). The computational resources and Biovia

Discovery Studio Client v17.2 software (Accelrys, San Diego, CA, USA), used for homology modeling and molecular docking studies, were provided through Croatian Science Foundation projects (grant numbers HrZZ-IP-2013-11-4307 and HrZZ-IP-2018-01-7683).

Appendix A. Supplementary data

Supplementary data to this article can be found online at https://doi.org/10.1016/j.tiv.2019.104713.

References

Allocati, N., Masulli, M., Di Ilio, C., Federici, L., 2018. Glutathione transferases: substrates, inihibitors and pro-drugs in cancer and neurodegenerative diseases. Oncogenesis. 7 (8).
Antizar-Ladislao, B., 2008. Environmental levels, toxicity and human exposure to tributyltin (TBT)-contaminated marine environment. A review. Environ. Int. 34, 292–308.
Bašica, B., Mihaljević, I., Maraković, N., Kovačevic, R., Smital, T., 2019. Molecular characterization of zebrafish Gstr1, the only member of teleost-specific glutathione S-transferase class. Aquat. Toxicol. 208, 196–207.
Copeland, R.A., 2005. Evaluation of Enzyme Inhibitors in Drug Discovery, Journal of Chemical Information and Modeling. A John Wiley & Sons, Inc., Hoboken, New Jersey.
de Araújo, J., Fernandez, P., Podratz, P.L., Merlo, E., Sarmento, I.V., da Costa, C.S., Niño, O.M.S., Faria, R.A., Freitas, L.L.C., Graceli, J.B., 2018. Organotin exposure and vertebrate reproduction: a review. Front. Endocrinol. 9, 64.
Di Giulio, R.T., Hinton, D.E., 2008. The Toxicology of Fishes. CRC Press ISBN 9780415248686.
Droge, W., 2002. Free radicals in the physiological control of cell function. Physiol. Rev. 82, 47–95.
Eaton, D.L., Bammler, T.K., 1999. Concise review of the glutathione S-transferases and their significance to toxicology. Toxicol. Sci. 49, 156–164.
Ema, M., Itami, T., Kawasaki, H., 1991a. Behavioral effects of acute exposure to tributyltin chloride in rats. Neurotoxicol. Teratol. 13, 489–493.
Ema, M., Itami, T., Kawasaki, H., 1991b. Changes of spontaneous motor activity of rats after acute exposure to tributyltin chloride. Drug Chem. Toxicol. 14, 161–171.
Fair, P.H., 1986. Interaction of benzo(a)pyrene and cadmium on GSH-S-transferase and benzo(a)pyrene hydroxylase in the black sea bass Centropristis striata. Arch. Environ. Contam. Toxicol. 15, 257.
Fang, L., Cuihong, X., Li, J., Borgghaard, O.K., Wang, D., 2017. The importance of environmental factors and matrices in the adsorption, desorption, and toxicity of butyltins: a review. Environ. Sci. Pollut. Res. 24, 9159–9173.
Fent, K., 1996. Ecotoxicology of organotin compounds. Crit. Rev. Toxicol. 26, 3–117.
Glisic, B., Mihaljevic, I., Popovic, M., Zaja, R., Loncar, J., Fent, K., Kovacevic, R., Smital, T., 2015. Characterization of glutathione-S-transferases in zebrafish (Danio rerio). Aquat. Toxicol. 158, 50–62.
Glisic, B., Hrubik, J., Fa, S., Dopudj, N., Kovacevic, R., Andric, N., 2016. Transcriptional profiles of glutathione-S-transferase isoforms, Cyp, and AOE genes in atrazine-exposed zebrafish embryos. Environ. Toxicol. 31.
Goodrich, J.M., Basu, N., 2012. Variants of glutathione s-transferase pi 1 exhibit differential enzymatic activity and inhibition by heavy metals. Toxicol. in Vitro 26 (4), 630–635.
Habig, W.H., Pabst, M.J., Jakoby, W.B., 1974. Glutathione S-transferases. The first enzymatic step in mercapturic acid formation. J. Biol. Chem. 249 (22), 7130–7139.
Hayes, J.D., Pulford, D.J., 1995. The glutathione S-transferase supergene family: regulation of GST and the contribution of the isoenzymes to cancer chemoprotection and drug resistance. Crit. Rev. Biochem. Mol. Biol. 30, 445–600.
Hayes, J.D., Flanagan, J.U., Jowsey, I.R., 2005. Glutathione transferases. Annu. Rev. Pharmacol. Toxicol. 45, 51–88.
Hoch, M., 2001. Organotin compounds in the environment – an overview. Appl. Geochem. 16, 719–743.
Ishihara, Y., Kawami, T., Ishida, A., Yamazaki, T., 2012. Tributyltin induces oxidative stress and neuronal injury by inhibiting glutathione S-transferase in rat organotypic hippocampal slice cultures. Neurochem. Int. 60 (8), 782–790.
Johansson, A.-S., Mannervik, B., 2002. Active-site residues governing high steroid isomerase activity in human glutathione transferase A3-3. J. Biol. Chem. 277, 16648–16654.
Kannan, K., Villeneuve, D.L., Blankenship, A.L., Giesy, J.P., 1998. Interaction of tributyltin with 3,3′,4,4′,5-pentachlorobiphenyl-induced ethoxyresorufin O-deethylase activity in rat hepatoma cells. J. Toxicol. Environ. Health A. 55 (5), 373–384.
Koska, J., Spassov, V.Z., Maynard, A.J., Yan, L., Austin, N., Flook, P.K., Venkatachalam, C.M., 2008. Fully automated molecular mechanics based induced fit protein-ligand docking method. J. Chem. Inf. Model. 48 (10), 1965–1973.
Lo, B.M., Oakley, A.J., Battistoni, A., Mazzetti, A.P., Nuccetelli, M., Mazzarese, G., Rossjohn, J., Parker, M.W., Ricci, G., 1997. Multifunctional role of Tyr108 in the catalytic mechanism of human glutathione transferase P1-1. Crystallographic and kinetic studies of the Y108F mutant enzyme. Biochemistry 36, 6207–6217.
Luk'yanova, O.N., Ireikina, S.A., 2011. Glutathione-S-transferase as a molecular biomarker of the state of marine organisms influenced by anthropogenic pressure. Biol. Bull. Russ. Acad. Sci. 38, 386.
Magi, E., Di Carro, M., 2016. Marine environment pollution: the contribution of mass spectrometry to the study of seawater. Mass Spectrom. Rev. 37, 492–512.
Marakovic, N., Knezevic, A., Vinkovic, V., Kovarik, Z., Sinko, G., 2016. Design and synthesis of N-substituted-2-hydroxyiminoacetamides and interactions with cholinesterases. Chem. Biol. Interact. 259, 122–132 Part B.
Matthiessen, P., Gibbs, P.E., 1998. Critical appraisal of the evidence for tributyltinmediated endocrine disruption in mollusks. Environ. Toxicol. Chem. 17, 37–43.
Mihaljevic, I., Popovic, M., Zaja, R., Marakovic, N., Sinko, G., Smital, T., 2017. Interaction between the zebrafish (Danio rerio) organic cation transporter 1 (Oct1) and endo- and xenobiotics. Aquat. Toxicol. 187, 18–28.
Nakatsu, Y., Kotake, Y., Komasaka, K., Hakozaki, H., Taguchi, R., Kume, T., Akaike, A., Ohta, S., 2006. Glutamate excitotoxicity is involved in cell death caused by tributyltin in cultured rat cortical neurons. Toxicol. Sci. 89, 235–242.
Oakley, A., 2011. Glutathione transferases: a structural perspective. Drug Metab. Rev. 43 (2), 138–151.
Oakley, A.J., Bello, M.L., Battistoni, A., Ricci, G., Rossjohn, J., Villar, H.O., Parker, M.W., 1997. The structures of human glutathione transferase P1-1 in complex with glutathione and various inhibitors at high resolution. J.Mol.Biol. 274, 84–100.
Oakley, A.J., Lo Bello, M., Nuccetelli, M., Mazzetti, A.P., Parker, M.W., 1999. The ligandin (non-substrate) binding site of human Pi class glutathione transferase is located in the electrophile binding site (H-site). J.Mol.Biol. 291, 913–926.
O'Callaghan, J.P., Miller, D.B., 1988. Acute exposure of the neonatal rat to tributyltin results in decreases in biochemical indicators of synaptogenesis and myelinogenesis. J. Pharmacol. Exp. Ther. 246, 394–402.
Păunescu, E., Soudani, M., Clavel, C.M., Dyson, P.J., 2017. Varying the metal to ethacrynic acid ratio in ruthenium(ii)/osmium(ii)-p-cymene conjugates. J. Inorg. Biochem. 175, 198–207.
Pesce, S.F., Cazenave, J., Monferrán, V.M., Frede, S., Wunderlin, D.A., 2008. Integrated survey on toxic effects of lindane on neotropical fish: Corydoras paleatus and Jenynsia multidentata. Environ. Pollut. 156 (3), 775–783.
Rossini, L., Jepson, I., Greenland, A.J., Gorla, M.S., 1996. Characterization of glutathione S-transferase isoforms in three maize inbred lines exhibiting differential sensitivity to Alachlor. Plant Physiol. 112 (4), 1595–1600.
Sali, A., Blundell, T.L., 1993. Comparative protein modelling by satisfaction of spatial restraints. J. Mol. Biol. 234 (3), 779–815.
Sheehan, D., Meade, G., Foley, V.M., Dowd, C.A., 2001. Structure, function and evolution of glutathione transferases: implications for classification of an ancient enzyme superfamily. Biochem. J. 360 (1), 16.
Shi, Y., Zhang, Q., Huang, D., Zheng, X., Shi, Y., 2016. Survival, growth, detoxifying and antioxidative responses of earthworms (Eisenia fetida) exposed to soils with industrial DDT contamination. Pestic. Biochem. Physiol. 128, 22–29.
Stäb, J.A., Traas, T.P., Stroomberg, G., van Kesteren, J., Leonards, P.E.G., van Hattum, A.G.M., Brinkman, U.A.T., Cofino, W.P., 1996. Determination of organotin compounds in the foodweb of a shallow freshwater lake in the Netherlands. Arch. Environ. Contam. Toxicol. 31, 319.
Stewart, R.K., Smith, G.B.J., Donnelly, P.J., Reid, K.R., Petsikas, D., Conlan, A.A., Massey, T.E., 1999. Glutathione S-transferase-catalyzed conjugation of bioactivated aflatoxin B1 in human lung: differential cellular distribution and lack of significance of the GSTM1 genetic polymorphism. Carcinogenesis. 20 (10), 1971–1977.
Tierbach, A., Groh, K.J., Schönenberger, R., Schirmer, K., Suter, M.J.F., 2018. Glutathione S-Transferase protein expression in different life stages of zebrafish (Danio rerio). Toxicol. Sci. 162, 702–712.
Triebskorn, R., Kohler, H.R., Flemming, J., Braunbeck, T., Negele, R.D., Rahmann, H., 1994. Evaluation of bis(tri-n-butyltin)oxide (TBTO) neurotoxicity in rainbow trout (Oncorhynchus mykiss). I. Behaviour, weight increase, and tin content. Aquat. Toxicol. 30, 189–197.
Wilce, M.C.J., Parker, M.W., 1994. Structure and function of glutathione S-transferases. Biochim. Biophys. Acta 1205, 1–18.
Yamada, J., Inoue, K., Furukawa, T., Fukuda, A., 2010. Low-concentration tributyltin perturbs inhibitory synaptogenesis and induces neuronal death in immature but not mature neurons. Toxicol. Lett. 198, 282–288.
Zhang, J., Zhenghong, Z., Rong, C., Yixin, C., Chonggang, W., 2008. Tributyltin exposure causes brain damage in Sebastiscus marmoratus. Chemosphere. 73, 337–343.
Zhang, J., Zhenghong, Z., Wenwen, Z., Ping, S., Chonggang, W., 2013. Sex-different effects of tributyltin on brain aromatase, estrogen receptor and retinoid X receptor gene expression in rockfish (Sebastiscus marmoratus). Mar. Environ. Res. 90, 113–118.